Photoelectron spectroscopy of C_4^-, C_6^-, and C_8^-

Cangshan Xu, Gordon R. Burton,[a] Travis R. Taylor, and Daniel M. Neumark
Department of Chemistry, University of California, Berkeley, California 94720 and Chemical Sciences Division, Lawrence Berkeley Laboratory, Berkeley, California 94720

(Received 7 March 1997; accepted 29 May 1997)

Photoelectron spectra of C_4^-, C_6^-, and C_8^- were obtained at two photodetachment wavelengths, 266 nm (4.657 eV) and 213 nm (5.822 eV). The spectra reveal considerably more electronic and vibrational structure than was seen in previous studies of these species [D. W. Arnold *et al.*, J. Chem. Phys. **95**, 8753 (1991)]. Term values for several low-lying excited electronic states of the neutral carbon clusters have been obtained, as well as new vibrational frequencies for the ground and some of the excited electronic states of the neutral clusters. The assignments of excited electronic states were aided by measurements of the photoelectron angular distributions. A new assignment of the vibrational frequencies for C_6 is in considerably better agreement with *ab initio* results than our original assignment. © *1997 American Institute of Physics.* [S0021-9606(97)01533-X]

I. INTRODUCTION

Small polyatomic carbon clusters have been of considerable interest to experimentalists and theoreticians for many years. Up until 1989, the spectroscopy of carbon clusters consisted primarily of matrix isolation studies; these are summarized in the excellent review of Weltner and van Zee.[1] Since then, high-resolution gas-phase infrared spectra have been measured for the linear carbon clusters C_3–C_9 and C_{13}, yielding rotational constants and some vibrational frequencies for the ground electronic states of these species.[2–8] Vibrational frequencies for several totally symmetric (and IR inactive) modes have been determined for several clusters using anion photoelectron spectroscopy and zero electron kinetic energy (ZEKE) spectroscopy.[9–11] Thus, the ground-state spectroscopy of linear carbon clusters is reasonably well characterized.

The low-lying excited electronic states of carbon clusters have received far less attention, even though electronic transitions in these species are of considerable interest as possible candidates for the diffuse interstellar bands.[4,12] This possibility has motivated studies by Maier and co-workers[13–15] in which visible and ultraviolet absorption spectra were obtained for a series of mass-selected anion and neutral carbon clusters in cryogenic matrices. However, *ab initio* calculations[16–21] predict the existence of additional lower-lying electronic states in linear carbon clusters, particularly for the open-shell species C_4, C_6, and C_8. Many of these states are optically inaccessible from the ground state of the neutral cluster, but they can be reached by photodetachment of the corresponding anion if the photon energy is sufficient. The anion photoelectron spectra measured by Yang *et al.* were obtained at a sufficiently high-photon energy to access excited states lying within 2–4 eV of the ground state, but due to the low resolution of these spectra no assignments were attempted.[22,23] In the higher-resolution anion photoelectron spectra obtained by Arnold *et al.*[9] several transitions were tentatively assigned to excited electronic states. However, the term values implied by these assignments were often comparable to vibrational frequencies of the cluster, making it difficult to distinguish transitions to excited electronic states from transitions to excited vibrational levels of the ground electronic state. In this study, we report anion photoelectron spectra of C_4^-, C_6^-, and C_8^- at photodetachment wavelengths of 266 nm (4.657 eV) and 213 nm (5.822 eV). The lower-photon energy was also used in our earlier study, but several modifications to the apparatus (see below) have resulted in higher quality spectra. The new spectra resolve some of the questions raised in *ab initio* calculations by Liu[24] and Botschwina[25] regarding our original assignments of vibrational frequencies in C_6 photoelectron spectrum. The spectra at 213 nm show a wealth of new transitions to excited vibrational levels and electronic states of the neutral clusters that are inaccessible at 266 nm. By combining the larger number of observed transitions with measurements of the photoelectron angular distributions, we can sort out most of the overlapped vibrational and electronic transitions seen in these spectra, thereby obtaining a detailed picture of the low-lying electronic states of the neutral clusters.

II. EXPERIMENT

The experiments were carried out on a time-of-flight negative ion photoelectron spectrometer. The original version of this instrument has been described in detail previously.[26] However, several modifications have been made since our previous study on carbon clusters.[9] The ion source was changed from a laser ablation/pulsed molecular beam source to a pulsed electrical discharge source.[27] The ion extraction electronics were modified so that the ion source no longer needs to be floated at high voltage. Finally, a reflectron stage has been added to improve the resolution

[a]Current address: Whiteshell Laboratories, Pinawa, Manitoba, ROE 1L0, Canada.

 0021-9606/97/107(9)/3428/9/$10.00

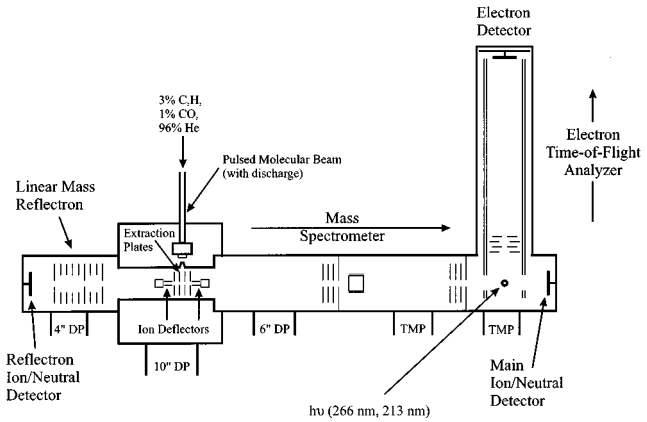

FIG. 1. Anion photoelectron spectrometer with linear mass reflectron.

of the time-of-flight mass spectrometer. The modified instrument is shown in Fig. 1 and the new features are described below.

The construction of the free jet pulsed discharge source is discussed elsewhere.[27] To make carbon cluster anions, a burst of a gas mixture (3% C_2H_2, 1% CO_2, and 96% Ne) from a piezo electric valve passes through two stainless steel plates, between which a high voltage (about 600 V) pulse is applied, and expands into a vacuum chamber. The resulting

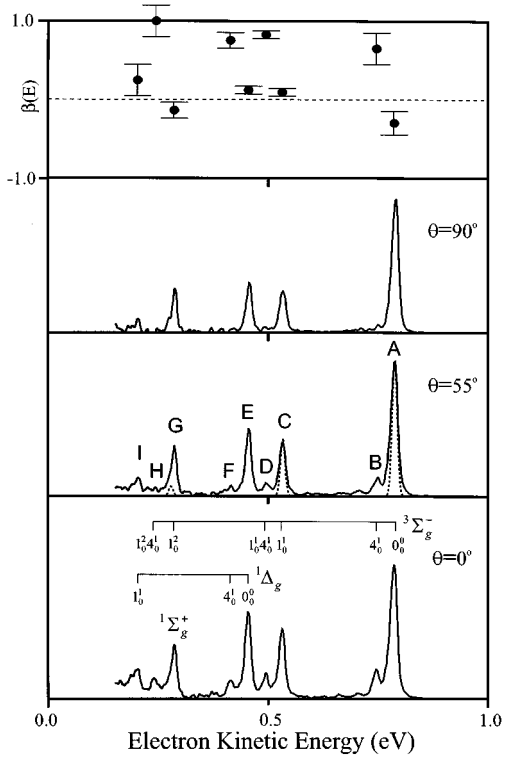

FIG. 2. Photoelectron spectra of C_4^- taken at photodetachment wavelength of 266 nm (4.657 eV). Laser polarization angles are θ=90°, 55°, and 0° with respect to direction of electron collection. Top panel shows anisotropy parameters $\beta(E)$ for several peaks in the spectra, plotted from −1 to 1 for greater clarity (β_{max}=2). The dotted line in the third panel shows a Franck–Condon simulation. Assignments are indicated in the bottom panel.

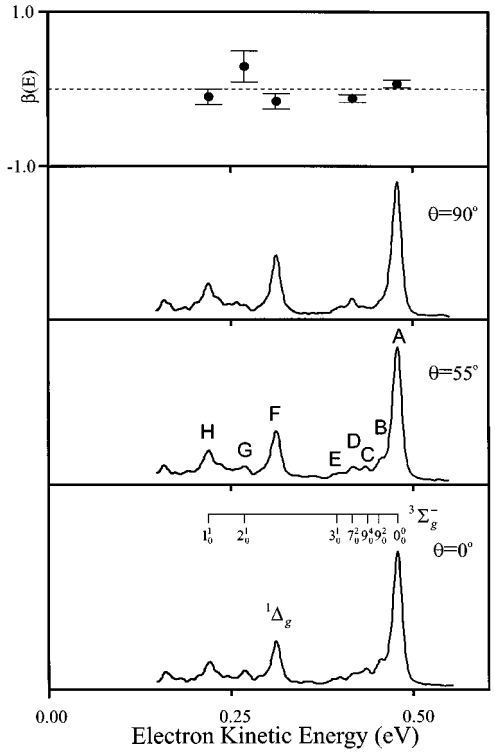

FIG. 3. Photoelectron spectra of C_6^- taken at 266 nm. Laser polarization angles are θ=90°, 55°, and 0° with respect to direction of electron collection. Top panel shows $\beta(E)$ parameters.

free jet is collimated by a 2 mm diam skimmer located 1.5 cm downstream from the nozzle and then enters a differentially pumped region. Here, the ions are extracted from the beam by applying a pulsed electric field across the two central plates shown in Fig. 1; the two outer plates are maintained at ground potential. Typically, pulses of −1500 and −1000 V with less than 100 ns rise times[28] are applied to the right and left central plates, respectively, resulting in a nominal ion beam energy of 1250 eV. Since both plates are pulsed simultaneously, it is no longer necessary to float the ion source at the nominal ion beam energy.

The extracted ions are mass-selected using a time-of-flight mass spectrometer with a newly added linear reflectron stage. A similar setup has been reported by Cheshnovsky and co-workers.[29] Although not necessary for this experiment, the reflectron stage increases our mass resolution from 150 to about 2000 by so-called ''second order focusing,''[30,31] which corrects the energy spread left over by the traditional Wiley–McLaren-type mass spectrometer.[32] A two-stage reflectron design[33] is used, consisting of seven stainless steel plates which form two uniform electric fields; these deceleration and reflection fields are defined by three plates, each with a 12.5 mm diam aperture covered with a fine grid. The front plate (closest to the extraction region) is grounded and progressively more negative dc voltages are applied to the middle and rear plates. The deceleration and reflection stages are 8 and 18 cm long, respectively. The other four plates have 25 cm diam apertures without grids and are connected by resistor chains in order to maintain uniform electric field

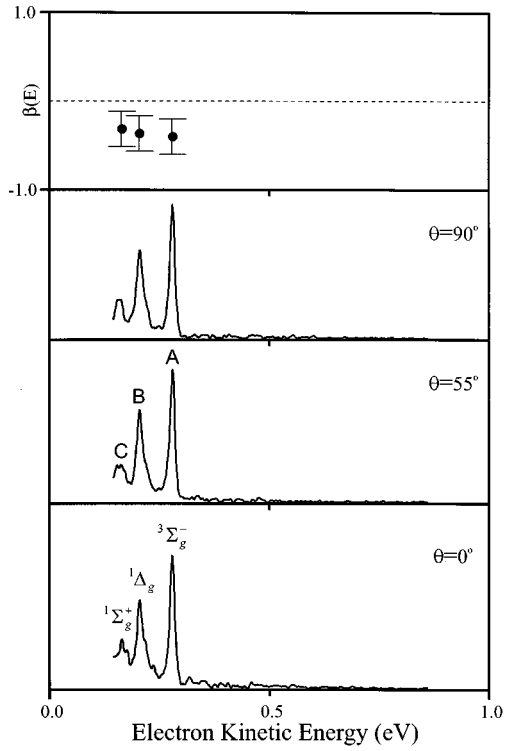

FIG. 4. Photoelectron spectra of C_8^- taken at 266 nm. Laser polarization angles are θ=90°, 55°, and 0° with respect to direction of electron collection. Top panel shows $\beta(E)$ parameters.

lines within each stage. Typical electric fields applied to a 1.25 keV ion beam are 125 and 50 V cm^{-1} in the deceleration and reflection stages, respectively.

The potentials of the extraction plates are reset to ground before the reflected ions pass through the second time on their way to the laser interaction region. The accelerated ions separate in time and space according to their mass to charge ratios and are selectively detached by a pulsed Nd:YAG laser.

Two different wavelengths, the fourth and fifth harmonics (266 nm, 4.657 eV, and 213 nm, 5.822 eV, respectively) from a pulsed Nd:YAG laser are used in these experiments. The photoelectron kinetic energy is measured by time-of-flight. The instrumental resolution is 8–10 meV for an electron kinetic energy (eKE) of 0.65 eV and degrades as $(eKE)^{3/2}$. The polarization angle θ between the laser polarization and the direction of electron collection can be varied using a half-wave plate. The variation of peak intensities with θ is used to separate the contributions of different electronic states to the photoelectron spectra.

Secondary electrons resulting from scattered photons create enough noise to necessitate background subtraction in the 213 nm spectra. This problem also exists to a considerably lesser extent in the 266 nm data.

III. RESULTS

The photoelectron spectra of C_4^-, C_6^-, and C_8^-, obtained at a photodetachment wavelength of 266 nm (4.657 eV) are presented in Figs. 2–4. The 213 nm (5.822 eV) spectra are shown in Fig. 5. Data were taken at laser polarization angles of 0°, 54.7° (magic angle) and 90° for all three clusters at both wavelengths. The spectral features correspond to the transitions between the anion electronic ground state and various neutral electronic states. For each peak, the electron kinetic energy (eKE) is given by

$$\mathrm{eKE} = h\nu - \mathrm{EA} - T_0^{(0)} + T_0^{(-)} - E_\nu^{(0)} + E_\nu^{(-)},$$

where $h\nu$ is the laser photon energy, EA is the adiabatic electron affinity of the neutral species, $T_0^{(0)}$ and $T_0^{(-)}$ are the term values of the neutral and anion electronic states, and $E_\nu^{(0)}$ and $E_\nu^{(-)}$ are the neutral and anion vibrational energies, respectively, above the zero-point energy. The peak positions at both photodetachment energies are listed in Table I.

From the changes in peak intensity with laser polarization angle, one obtains information on the photoelectron angular distribution associated with each peak. This is given by[34]

$$\frac{d\sigma}{d\Omega} = \frac{\sigma_{\mathrm{total}}}{4\pi}\left[1 + \beta(E) P_2(\cos\,\theta)\right],$$

where σ_{total} is the total photodetachment cross section and $\beta(E)$ is the asymmetry parameter. $\beta(E)$ varies between -1 and 2; these limits correspond to $\sin^2\theta$ and $\cos^2\theta$ distributions, respectively. One can therefore determine β for each peak in the photoelectron spectrum. The results are shown in Table I with the peak positions, and plotted in the top panels (for the major peaks) of Figs. 2–5.

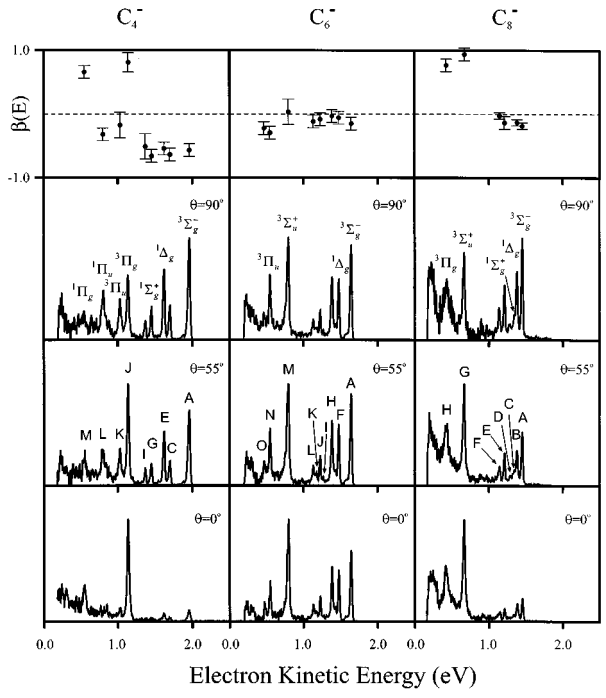

FIG. 5. Photoelectron spectra of C_4^-, C_6^- and C_8^- taken at photodetachment wavelength of 213 nm (5.822 eV). Laser polarization angles are θ=90°, 55°, and 0° with respect to direction of electron collection. Top panel shows $\beta(E)$ parameters for several peaks. Low-lying electronic state assignments are indicated in the second panel.

TABLE I. Peak positions and assignments for the C_4^-, C_6^-, and C_8^- photoelectron spectra.

		Position (eV)		$\beta(E)$		
Molecule	Peak	266 nm	213 nm	266 nm	213 nm	Assignments
C_4	A	0.787	1.960	−0.30±0.15	−0.57± 0.10	$^3\Sigma_g^-$ Origin
	B	0.747	1.882	0.65±0.20		$4_0^1(^3\Sigma_g^-)$
	C	0.532	1.700	0.09±0.05	−0.64± 0.10	$1_0^1(^3\Sigma_g^-)$
	D	0.495		0.83±0.05		$1_0^1 4_0^1(^3\Sigma_g^-)$
	E	0.455	1.621	0.12±0.05	−0.54± 0.10	$^1\Delta_g$ Origin
	F	0.414		0.76±0.10		$4_0^2(^1\Delta_g)$
	G	0.286	1.454	−0.14±0.10	−0.66± 0.10	$1_0^2(^3\Sigma_g^-)$, $^1\Sigma_g^+$ Origin
	H	0.243		1.00±0.20		$1_0^2 4_0^1(^3\Sigma_g^-)$
	I	0.203	1.370	0.25±0.20	−0.51± 0.20	$1_0^1(^1\Delta_g)$
	J		1.140		0.81± 0.15	$^3\Pi_g$ Origin
	K		1.032		−0.17± 0.20	$^3\Pi_u$ Origin
	L		0.800		−0.32± 0.10	$1_0^1(^3\Pi_u)$, $^1\Pi_u$ Origin
	M		0.548		0.66± 0.10	$^1\Pi_g$ Origin
C_6	A	0.479	1.645	0.07±0.05	−0.15± 0.10	$^3\Sigma_g^-$ Origin
	B	0.457				$9_0^2(^3\Sigma_g^-)$
	C	0.435				$9_0^4(^3\Sigma_g^-)$
	D	0.418		−0.12±0.05		$7_0^2(^3\Sigma_g^-)$
	E	0.400				$3_0^1(^3\Sigma_g^-)$
	F	0.313	1.475	−0.16±0.10	−0.06± 0.10	$^1\Delta_g$ Origin
	G	0.269	1.433	0.29±0.20	−0.05± 0.20	$2_0^1(^3\Sigma_g^-)$
	H	0.220	1.384	−0.10±0.10	−0.03± 0.10	$1_0^1(^3\Sigma_g^-)$
	I		1.266		−0.26± 0.10	$2_0^1(^1\Delta_g)$
	J		1.225		−0.08± 0.10	$1_0^1(^1\Delta_g)$
	K		1.174		−0.02± 0.05	$1_0^1 2_0^1(^3\Sigma_g^-)$
	L		1.132		−0.12± 0.10	$1_0^2(^3\Sigma_g^-)$
	M		0.796		0.03± 0.20	$^3\Sigma_u^+$ Origin
	N		0.547		−0.29± 0.10	$^3\Pi_u$ Origin
	O		0.467		−0.22± 0.10	$3_0^1(^3\Pi_u)$
C_8	A	0.280	1.450	−0.40±0.20	−0.18± 0.05	$^3\Sigma_g^-$ Origin
	B	0.205	1.379	−0.37±0.20	−0.13± 0.05	$^1\Delta_g$ Origin
	C	0.165	1.341	−0.32±0.20	−0.06± 0.10	$^1\Sigma_g^+$ Origin
	D		1.281		−0.03± 0.10	$3_0^1(^3\Sigma_g^-)$
	E		1.211		−0.13± 0.10	$1_0^1(^3\Sigma_g^-)$ and $3_0^1(^1\Delta_g)$
	F		1.143		−0.02± 0.05	$1_0^1(^1\Delta_g)$
	G		0.667		0.94±0.10	$^3\Sigma_u^+$ Origin
	H		0.423		0.77± 0.10	$^3\Pi_g$ Origin

We first consider the photoelectron spectra. In all of the 266 nm spectra, the largest peak occurs at the highest electron energy. This is the vibrational origin transition between the electronic ground states of the anion and neutral and from this one obtains the adiabatic electron affinity. The electron affinities from the new spectra are unchanged from our previous work.[9,10] In comparison to our previous results[9] at 266 nm, several of the peaks are better resolved in the current work, and more features are seen at low eKE. In the C_4^- spectra, peaks F, G, H, and I are new features which were not observed previously. In the earlier C_6^- spectra, peak A had a wide shoulder towards lower electron energy. This is now resolved as a series of peaks (B–E). Peaks F and G (formerly D and E) are better resolved and peak H is a new feature. In the C_8^- spectra, peak C is a new feature.

The 213 nm spectra show many more peaks than the 266 nm spectra, corresponding to higher energy levels of the neutral species. For peaks appearing in both spectra, however, the energy resolution is poorer at 213 nm because the electron kinetic energy is higher. The most noticeable difference in the 213 nm spectra is that a new peak at lower eKE is the largest feature for all three species. This is peak *J* in the C_4^- spectra, peak M in the C_6^- spectra, and peak G in the C_8^- spectra. Although some peaks at low eKE are not very well resolved due to the low signal-to-noise ratio, we are still able to identify most of them by comparing the three spectra at different polarization angles.

The laser polarization results for C_4^- show substantial variation in the photoelectron angular distribution among the peaks. At 266 nm, we find $\beta=0$ for the major peaks (A,C,E,G,I), but the photoelectron angular distributions for several of the smaller peaks (B,D,F,H) are considerably more

TABLE II. Calculated and experimental energies[a] of C_4 low-lying electronic states (eV).

Method/Basis set	$^3\Sigma_g^-$	$^1\Delta_g$	$^1\Sigma_g^+$	$^3\Pi_g$	$^1\Pi_g$	$^3\Pi_u$	$^1\Pi_u$
MBPT(4)/DZP[b]	0.0	0.25	0.256	0.84		1.15	
CC/DZP[b]	0.0			0.97		1.30	
MRD CI/DZP[c]	0.0	0.41	0.68	1.00	1.73	1.54	2.05
CISD with Davidson's correction[d]	0.0	0.33	0.40[e]				
UHF/FOCO/CC[f]	0.0	0.40		0.96		1.26	
10-CAS/G[4421][g]	0.0	0.30	0.42				
10-MRCI/G[4421][g]	0.0	0.35					
MP2/6-31G*[h]	0.0			0.46	0.71	0.75	1.06
UV-PES[h]	0.0	0.332	0.50	0.82	1.41	0.93	1.16

[a]Vertical excitation energies except for the present work which indicates adiabatic energies.
[b]Reference 16.
[c]Reference 19.
[d]Reference 17.
[e]A mixture of the $^1\Sigma_g^+$ and $^1\Delta_g$ singlet states.
[f]Reference 20.
[g]Reference 18.
[h]Present work. Error bars from photoelectron spectra assignments are ± 0.02 eV except for the $^1\Delta_g$ state of ± 0.015 eV.

anisotropic with $\beta \approx 1$. At 213 nm, the anisotropy parameters cluster about three values. We find β has dropped from 0 to -0.6 for peaks A,C,E,G, and I, $\beta \approx -0.25$ for peaks K and L, and $\beta \approx 0.75$ for peaks J and M. There is considerably less variation among the β values for the peaks in the C_6^- spectra. At 266 nm, all the features are essentially isotropic with $\beta \approx 0$. The same is true at 213 nm, except for peaks N and O for which $\beta \approx -0.25$. The results at 213 nm for C_8^- show that β lies between -0.03 and -0.18 for peaks A–F, but that peaks G and H have considerably more anisotropic distributions with $\beta = 0.94$ and 0.77, respectively.

The polarization dependence results clearly show that transitions to multiple electronic states contribute to the photoelectron spectra. In order to help assign these transitions, we performed geometry optimization and frequency calculations on various electronic states at the HF/6-31G* and MP2/6-31G* levels of theory, using the GAUSSIAN 92 package.[35] Franck–Condon simulations can be performed using the geometries and force constants obtained from the calculation. The adiabatic excitation energies from our calculations and results from previous *ab initio* studies are summarized in Tables II–IV. Note that the $^3\Sigma_u^+$ state that we have calculated is a cumulenic state in which all the carbon atoms are connected by double bonds, in contrast to the low-lying polyacetylenic $^3\Sigma_u^+$ state predicted in some of the calculations.[17,21]

TABLE III. Calculated and experimental energies[a] of C_6 low-lying electronic states (eV).

Method/Basis set	$^3\Sigma_g^-$	$^1\Delta_g$	$^1\Sigma_g^+$	$^3\Sigma_u^+$	$^3\Pi_u$
10-CAS[b]	0.0	0.30	0.53		
10-MCRI[b]	0.0	0.15	0.28		
CISD with Davidson's correction[c]	0.0	0.19	0.16[d]		
MP2/6-31G*[e]	0.0			1.00	1.20
UV-PES[e]	0.0	0.166		0.85	1.10

[a]Vertical excitation energies except for the present work which indicates adiabatic energies.
[b]Reference 21.
[c]Reference 17.
[d]A mixture of the $^1\Sigma_g^+$ and $^1\Delta_g$ singlet states.
[e]Present work. Error bars from photoelectron spectra assignments are ± 0.02 eV except for the $^1\Delta_g$ state of ± 0.015 eV.

IV. ANALYSIS AND DISCUSSION

A. General

In this section we review the electronic structure of C_4, C_6, C_8, and their anion counterparts. We then discuss strategies for assigning the various electronic transitions that comprise the photoelectron spectra.

The ground-state molecular orbital configurations for the three anions are: $\cdots(1\pi_u)^4(4\sigma_u)^2(5\sigma_g)^2(1\pi_g)^3$ for C_4^-,[36] $\cdots(1\pi_u)^4(6\sigma_u)^2(7\sigma_g)^2(1\pi_g)^4(2\pi_u)^3$ for C_6^-,[37] and $\cdots(8\sigma_u)^2(9\sigma_g)^2(2\pi_u)^4(2\pi_g)^3$ for C_8^-,[38] yielding $^2\Pi_g$ ground states for C_4^- and C_8^- and a $^2\Pi_u$ ground state for C_6^-. In each case, removal of an electron from the highest occupied molecular orbital (HOMO) leaves a neutral cluster with a π^2 configuration, resulting in a $^3\Sigma_g^-$ ground state and the low-lying $^1\Delta_g$ and $^1\Sigma_g^+$ excited states. Thus, all three states are accessible via one-electron photodetachment transitions from the anions. Higher-lying excited states can be formed by removal of electrons from orbitals other than the HOMO,

TABLE IV. Calculated and experimental energies[a] of C_8 low-lying electronic states (eV).

Method/Basis set	$^3\Sigma_g^-$	$^1\Delta_g$	$^1\Sigma_g^+$	$^3\Sigma_u^+$	$^3\Pi_u$
CISD with Davidson's correction[b]	0.0	0.14	0.01[c]		
MP2/6-31G*[d]	0.0			1.45	1.53
UV-PES[d]	0.0	0.071	0.115	0.78	1.03

[a]Vertical excitation energies except for the present work which indicates adiabatic energies.
[b]Reference 17.
[c]A mixture of the $^1\Sigma_g^+$ and $^1\Delta_g$ singlet states.
[d]Present work. Error bars from photoelectron spectra assignments are ± 0.015 eV for the $^1\Delta_g$ and $^1\Sigma_g^+$ states and ± 0.02 eV for the others.

TABLE V. Adiabatic excitation energies (eV) of C_4, C_6, and C_8 low-lying states from present work.

	$T_0(^1\Delta_g)$	$T_0(^1\Sigma_g^+)$	$T_0(^3\Sigma_u^+)$	$T_0(^3\Pi_g)$	$T_0(^3\Pi_u)$	$T_0(^1\Pi_u)$	$T_0(^1\Pi_g)$
C_4	0.332	0.93		0.82	0.93	1.16	1.41
C_6	0.166		0.85		1.10		
C_8	0.071	0.115	0.78	1.03			

yielding for example, triplet and singlet Π_g and Π_u states of C_4, and $^3\Sigma_u^+$ state for C_6 and C_8. According to the *ab initio* results listed in Tables II–IV, many of these states will be accessible by photodetachment at 213 nm. In order to assign the observed transitions, we use the anisotropy parameters β described in the previous section and *ab initio* vibrational frequencies and term values.

The photoelectron angular distributions are determined by the distribution of partial waves contributing to each peak. The relevant selection rules for these near threshold are straightforward; for a linear, centrosymmetric molecule, *s*-wave ($l=0$) detachment can occur from orbitals of *u* symmetry, but *p*-wave ($l=1$) detachment is the lowest allowed partial wave from orbitals of *g* symmetry.[39] Pure *s*-wave detachment yields an isotropic ($\beta=0$) angular distribution, whereas pure *p*-wave detachment leads to a $\cos^2\theta$ distribution with $\beta=2$.[40] As examples, C_6^- can undergo *s*-wave detachment near the threshold whereas C_4^- and C_8^- cannot. The situation is more complicated in photoelectron spectroscopy, however, because one is typically well above the detachment threshold for a particular neutral←anion transition, so that many partial waves typically contribute to the signal. One still has the restrictions that only even partial waves result from a *u* orbital, and only odd partial waves from a *g* orbital, but it is difficult to predict in advance the value of β for a photodetachment transition.

Nonetheless, one does expect relatively small variations in β for photodetachment transitions within an electronic manifold or for transitions between states with the same orbital configurations, because detachment from the same orbital in the anion is occurring. Thus, for example, transitions involving removal of an electron from the anion HOMO to yield the $^3\Sigma_g^-$ ground state $^1\Delta_g$ and $^1\Sigma_g^+$ excited states should have approximately the same values of β. This is in fact observed in the photoelectron spectrum of O_2^-,[41] where the symmetries of the states involved are the same as for carbon clusters: O_2^- has a $^2\Pi_g$ ground state, and O_2 has a $^3\Sigma_g^-$ ground state and $^1\Delta_g$ and $^1\Sigma_g^+$ excited states. Conversely, peaks with significantly different values of β should be associated with different electronic transitions. This is a useful diagnostic for distinguishing transitions between different electronic states from those involving vibrational transitions within the same electronic manifold, and it can also indicate the presence of vibronic coupling between electronic states of different symmetry (see below). However, one cannot assume that peaks with the same value of β belong to the same electronic transition, or even to transitions involving detachment from orbitals of the same symmetry. The photoelectron angular distributions are therefore useful in assigning the photoelectron spectra, but are by no means unambiguous. We therefore tend to minimize the number of electronic states needed to describe the spectrum so long as this does not lead to unreasonable vibrational frequencies. The term values obtained from our assignments of the photoelectron spectra are summarized in Table V.

B. C_4

C_4 has two totally symmetric stretching modes (ν_1 and ν_2), one σ_u antisymmetric stretch (ν_3), and two degenerate bending modes of π_g and π_u symmetry (ν_4 and ν_5, respectively). In our previous study of C_4^-, peaks A–D were assigned to the $^3\Sigma_g^-$ ground-state vibrational origin, 4_0^1, 1_0^1, and $1_0^1 4_0^1$ transitions.[9] These assignments were aided by vibrational frequencies from *ab initio* calculations.[42–44] The ν_4 (π_g) mode is not totally symmetric, so the 4_0^1 and $1_0^1 4_0^1$ transitions are Franck–Condon forbidden. However, the 4_0^1 transition can occur in the case of vibronic coupling to a nearby Π_g electronic state; this is discussed further below. Peak E was assigned as the origin of the first excited state $^1\Delta_g$ because the splitting between peaks A and E, 2680 cm^{-1}, is too large for a vibrational frequency of C_4.

While these assignments are still valid, the new spectra give slightly different vibrational frequencies: $\nu_1=2057\pm50$ cm^{-1} and $\nu_4=323\pm50$ cm^{-1}. The new term value of $T_0(^1\Delta_g)=0.332\pm0.015$ eV is in good agreement with the calculated values of 0.346 and 0.331 eV by Almlof[18] and Schaefer,[17] respectively (see Table II). Based on these ν_1 and ν_4 frequencies, the new features, peak G and H, are assigned to the 1_0^2 and $1_0^2 4_0^1$ transitions of the $^3\Sigma_g^-$ ground state. Peaks F and I are assigned to the 4_0^1 and 1_0^1 transitions of the $^1\Delta_g$ state, respectively. This yields a symmetric stretch frequency of $\nu_1=2032\pm50$ cm^{-1} and a bending frequency of $\nu_4=331\pm50$ cm^{-1} for the $^1\Delta_g$ state, which are very close to those of the ground state. Peak I is quite weak in the 266 nm spectrum due to the low-energy cutoff of the spectrometer.

Peak G lies at the energy expected for the 1_0^2 transition to the $^3\Sigma_g^-$ state, but its intensity is anomalously high. This is demonstrated in the third panel of Fig. 2, which shows a Franck–Condon simulation of the C_4^- photoelectron spectrum. The neutral geometry is adopted from the CCSD(T)/PVTZ calculation by Watts and Bartlett,[45] and the anion geometry is from the RCCSD(T) calculation by Schmatz and Botschwina.[46] The force constants from our MP2/6-31G* calculation have been applied to obtain the normal coordinate change between the anion and neutral. Since the 4_0^1 transition is not Franck–Condon allowed, only excitation of the ν_1 mode appears in the simulation, which shows that that the actual intensity of peak G is about five times higher than

predicted in the simulation. It is possible that the anomalous intensity of peak G arises because it is in part due to the transition to the $^1\Sigma_g^+$ state. As shown in Table II, calculations by Koutecký[19] and Almlöf[18] predict vertical excitation energies of 0.68 and 0.42 eV, respectively, for this state; these values bracket the experimental spacing of 0.50 eV between peaks A and G. We therefore tentatively assign peak G to a combination of the $^1\Sigma_g^+$ state origin and the 1_0^2 transition from the ground state, yielding a term energy of $T_0(^1\Sigma_g^+)=0.50\pm0.02$ eV.

All of the major peaks discussed thus far have approximately the same anisotropy parameter. Peak J in the 213 nm spectrum is the first large peak that shows a significantly different polarization dependence. We assign it to the lowest electronic state of C_4 which can be accessed by removing an electron from an orbital other than the HOMO. From Table II, theoretical calculations have predicted this to be the $^3\Pi_g$ state with a term value between 0.8 to 1 eV;[16,19] the photodetachment transition involves removal of a $5\sigma_g$ electron. Assigning peak J to this state yields a term energy of $T_0(^3\Pi_g)=0.82\pm0.02$ eV. Peak J has the same polarization dependence as peaks B, D, F, and H, which supports the earlier claim that these latter peaks occur due to vibronic coupling between the $^3\Sigma_g^-$ and $^1\Delta_g$ states via the ν_4 mode to a nearby $^3\Pi_g$ state.

Based on their anisotropies, peaks K and L clearly are associated with a different electronic transition than peak J. We therefore assign peak K to the transition to the $^3\Pi_u$ state of C_4 in which a $4\sigma_u$ electron is removed from the anion; this should be the next excited electronic state with a molecular orbital configuration that differs from the $^3\Pi_g$ state. Our assignment yields a term energy of $T_0(^3\Pi_u)=0.93$ eV for this state, a somewhat lower value than the previously calculated vertical excitation energies of 1.15 and 1.54 eV by Bartlett[16] and Koutecký,[19] respectively. Peak L is more problematic. It can be assigned as the 1_0^1 transition within the $^3\Pi_u$ manifold, yielding a symmetric stretch frequency of $\nu_1=1871\pm50\ \mathrm{cm}^{-1}$ for the $^3\Pi_u$ state. While this is a reasonable vibrational frequency, peaks K and L have the same intensity, which implies a significant normal coordinate change of the ν_1 mode upon photodetachment to this state. This disagrees with the trend followed by every other photodetachment transition in linear carbon clusters in which the 0_0^0 transition is the most intense. Alternatively, peak L could be the transition to the $^1\Pi_u$ state, as this should have approximately the same intensity and polarization dependence as the transition to the $^3\Pi_u$ state. This assignment implies $T_0(^1\Pi_u)=1.16\pm0.02$ eV and a singlet–triplet splitting of 0.23 eV. This splitting is somewhat smaller than the value of 0.50 eV calculated by Koutecký,[19] but agrees well with our MP2/6-31G* calculations which predict a singlet–triplet splitting of 0.31 eV. In any case, the assignment of peak L to the $^1\Pi_u$ state is certainly reasonable, but somewhat tentative.

Although peak M is not well resolved due to low signal-to-noise, it is the only other peak in the 213 nm spectrum with a similar anisotropy parameter as peak J. Since the splitting between peaks M and J is too large to assign peak M to a vibrational transition, we assign peak M to the transition to the $^1\Pi_g$ state in which, as with peak J, a $4\sigma_g$ electron is detached. This yields a singlet–triplet splitting of 0.59 eV and term energy of $T_0(^1\Pi_g)=1.41\pm0.02$ eV, slightly smaller than the vertical term energy of 1.73 eV predicted by Pacchioni and Koutecký.[19]

C. C_6

We have previously studied C_6^- using photoelectron spectroscopy[9] and a combination of autodetachment and zero electron kinetic energy (ZEKE) spectroscopy.[11] In this earlier work, the peaks now labeled A, F, and G were assigned to the vibrational origin, 3_0^1, and 2_0^1 photodetachment transitions of the $^3\Sigma_g^-$ ground state of C_6. The latter two assignments yielded vibrational frequencies of 492 and 1339 cm^{-1} for the ν_3 and ν_2 symmetric stretches, respectively. Both values are substantially lower than *ab initio* harmonic frequencies[24,25,47] which, for example, are calculated by Botschwina[25] to be 653 and 1697 cm^{-1}. The new features observed in the current work now lead to an assignment more in line with the *ab initio* values.

Peak H in the 266 nm spectrum at eKE 0.22 eV is $2089\pm50\ \mathrm{cm}^{-1}$ from the origin. We assign it to the 1_0^1 transition of the $^3\Sigma_g^-$ ground state, in good agreement with the *ab initio* value[25] of $\nu_1=2142\pm50\ \mathrm{cm}^{-1}$ and the previously observed peak in the ZEKE spectrum[11] at $2061\pm10\ \mathrm{cm}^{-1}$. Peak E, which was not observed previously, and peak G, which is considerably better resolved than in our previous photoelectron spectrum, lie $637\pm50\ \mathrm{cm}^{-1}$ and $1694\pm50\ \mathrm{cm}^{-1}$, respectively, from the origin, and assigning these to the 3_0^1 and 2_0^1 transitions yields vibrational frequencies in much better agreement with the *ab initio* values. Moreover, the relative intensities of peaks E, G, and H are in qualitative accord with the Franck–Condon simulation calculated by Botschwina.[25] Based on these new assignments, peaks K and L in the 213 nm spectrum are assigned to the $1_0^1 2_0^1$ and 1_0^2 transitions of the C_6 $^3\Sigma_g^-$ state.

The smaller peaks B, C, and D near the origin could be from even Δv transitions involving the low-frequency π bending modes or from sequence bands, with the latter being less likely due to the absence of hot band transitions at higher eKE than the origin. Even Δv transitions in nontotally symmetric vibrations can be observed if the change in frequency between the anion and neutral is large. Our MP2/6-31G* calculation yields $\nu_7(\pi_g)$ and $\nu_9(\pi_u)$ frequencies of 124 and 278 cm^{-1} for the anion, and 197 and 105 cm^{-1} for the neutral. Based on these large frequency changes, peaks B and C are assigned to the 9_0^2 and the 9_0^4 transitions, respectively, and peak D is assigned to the 7_0^2 transition. The resulting vibrational frequencies, $\nu_7=246\pm50\ \mathrm{cm}^{-1}$ and $\nu_9=90\pm50\ \mathrm{cm}^{-1}$, are in reasonable agreement with our *ab initio* values as well as those of a previous calculation.[48] Note that three peaks analogous to peaks B, C, and D were seen in the autodetachment spectrum[11] of C_6^-; these were labeled b_0, c_0, and d_0, and should be reassigned to the 9_0^2, 9_0^4, and 7_0^2 autodetachment transitions, respectively.

The second largest feature in the 266 nm spectrum is

peak F, which was assigned to the 2_0^1 transition in our previous study. Given our new assignment of peak G to this transition, peak F is assigned to the origin of the $^1\Delta_g$ excited state and peaks I and J in the 213 nm spectrum to the corresponding 2_0^1 and 1_0^1 transitions. The resulting term energy $T_0(^1\Delta_g)=0.166\pm0.015$ eV is in good agreement with the *ab initio* values of 0.15 and 0.19 eV calculated by Almlöf[21] and Schaefer,[17] respectively. This assignment provides two symmetric stretch frequencies of the $^1\Delta_g$ state, $\nu_1=2016\pm50$ cm^{-1} and $\nu_2=1686\pm50$ cm^{-1}, which are very close to their $^3\Sigma_g^-$ state counterparts.

We next consider the remaining peaks M, N, and O. These clearly correspond to transitions to one or more excited states of C_6, but since the anisotropy parameters are approximately the same (≈0) for all the C_6^- transitions, the excited-state assignments are more ambiguous than for C_4^-. Peak M, which lies 0.849 eV from peak A; is the most intense feature in the spectra and is readily assigned to the origin of an excited state. This could be the $^1\Sigma_g^+$ state which has the same $\cdots(1\pi_g)^4(2\pi_u)^2$ configuration as the $^3\Sigma_g^-$ and $^1\Delta_g$ states, or the $^3\Sigma_u^+$ state resulting from the $\cdots(1\pi_g)^3(2\pi_u)^3$ configuration. The term energy for the $^1\Sigma_g^+$ state has been calculated at the MRCI level by Almlöf[21] and found to be 0.28 eV, a considerably lower value than the experimental A–M spacing. The term energy for the $^3\Sigma_u^+$ state from our MP2/6-31G* level calculation is 1.20 eV. Furthermore, peak M has a somewhat different polarization dependence from peaks associated with the $^3\Sigma_g^-$ and $^1\Delta_g$ states; peak M is clearly more intense than peak A at $\theta=0°$ but has the same intensity at the other two angles. We therefore assign peak M to the $^3\Sigma_u^+$ state.

Peaks N and O are separated by 640 ± 50 cm^{-1}. They have the same polarization dependence but differ sufficiently from peak M to warrant their assignment to transitions to a different electronic state. The $^3\Pi_u$ state is the next triplet state expected above the $^3\Sigma_u^+$ state. Assigning peak N to the origin of this state yields $T_0(^3\Pi_u)=1.10\pm0.02$ eV, very close to our MP2/6-31G* value of 1.20 eV. This calculation also yields ν_3 (σ_g)$=642$ cm^{-1}, so we assign peak O to the 3_0^1 transition of the $^3\Pi_u$ state manifold.

The $^1\Sigma_g^+$ manifold has not been identified in the above assignments. There are several small unassigned peaks in the 266 nm spectrum near eKE$=0.25$ eV. This is the energy range where transitions to the $^1\Sigma_g^+$ state are expected,[21] and these small peaks may be due to this state. If so, it remains an open question as to why the cross section for photodetachment to the $^1\Sigma_g^+$ state is considerably smaller than for the $^3\Sigma_g^-$ and $^1\Delta_g$ states.

D. C_8

In our previous study[9] of C_8^-, the high electron affinity of C_8 (4.379 ± 0.006 eV) limited the amount of information obtained at 266 nm, and only peaks A and B were observed. Peak A was assigned to the origin of the $^3\Sigma_g^-$ ground state, where peak B was tentatively assigned to the 4_0^1 transition. The possible assignment of peak B to the $^1\Delta_g$ state was also proposed. The new results at 266 and 213 nm provide a considerably more complete assignment of the electronic and vibrational states of C_8. These assignments are aided by a recent high-level calculation by Schmatz and Botschwina[49] in which vibrational term energies (including anharmonicities) for levels involving the four totally symmetric stretches were calculated for the anion and the neutral ground state. A Franck–Condon simulation of the anion photoelectron spectrum was also carried out in that paper.

The assignment of peak A is unchanged. According to Botschwina's simulation, the strongest vibrational transition other than the origin should be the 1_0^1 (2053 cm^{-1}/24%) transition, followed by the 3_0^1 (1357 cm^{-1}/13%) transition. Peaks D and E lie 1361 and 1928 cm^{-1} from the origin, respectively. Peak D is therefore assigned to the 3_0^1 transition. While the A–E spacing is actually closer to the calculated energy of the ν_2 level (1977 cm^{-1}), the intensity of the 2_0^1 transition in the simulated photoelectron spectrum is negligible, and we assign peak E to the 1_0^1 transition.

The assignment of peak B to the 4_0^1 transition yields $\nu_4=605$ cm^{-1}, which is significantly larger than the calculated value of 500 cm^{-1}.[49] In addition, the 4_0^1 transition is calculated to have only 2% of the intensity of the origin, whereas peak B is about 70% as intense as peak A. We therefore assign peak B to the $^1\Delta_g$ excited electronic state, yielding a term energy of $T_0(^1\Delta_g)=0.071\pm0.015$ eV. This is somewhat smaller than the value of 0.141 eV calculated by Schaefer,[17] but the deviation is only slightly larger than for C_6. The decreasing $^3\Sigma_g^- - ^1\Delta_g$ splitting as the number of carbon atoms increases (Table V) is also consistent with the trend seen in Schaefer's calculation.[17] Peak F lies 0.236 eV from peak B, close to the spacing between peaks A and E (0.239 eV), and is assigned to the 1_0^1 transition of the $^1\Delta_g$ excited state, yielding $\nu_1=1903\pm50$ cm^{-1} for the $^1\Delta_g$ state. The splitting between peaks B and E is 1355 cm^{-1}, virtually identical to the ν_3 frequency in the $^3\Sigma_g^-$ state. It is therefore likely that the 3_0^1 transition in the $^1\Delta_g$ state manifold contributes to the intensity of peak E.

Peak C is 0.115 eV (927 cm^{-1}) from the $^3\Sigma_g^-$ state origin, and only 0.040 eV (322 cm^{-1}) from the $^1\Delta_g$ state origin. Within the ground-state manifold, the closest calculated vibrational energy level involving totally symmetric modes only is the $2\nu_4$ level (999 cm^{-1}), but the intensity of the 4_0^2 transition should be negligible. The splitting between peaks B and C is too small for peak C to be a transition to a symmetric stretch level of the $^1\Delta_g$ state. We therefore assign peak C to the origin of the $^1\Sigma_g^+$ state, yielding a term energy of $T_0(^1\Sigma_g^+)=0.115\pm0.015$ eV.

The two peaks at lowest eKE, peaks G and H, have anisotropy parameters close to one, in contrast to the nearly isotropic angular distributions at 213 nm for the other peaks. The first excited state with a different molecular orbital configuration from the ground state should be the $^3\Sigma_u^+$ cumulenic state, which can be accessed by detachment of a $2\pi_u$ electron from C_8^-, and the next triplet state should be the $^3\Pi_g$ state, accessible by detachment of a $9\sigma_g$ electron. Our MP2/6-31G* level calculations yield term energies of 1.45 and 1.53 eV for the $^3\Sigma_u^+$ and $^3\Pi_g$ states, respectively. We

assign peak G to the $^3\Sigma_u^+$ state origin, yielding $T_0(^3\Sigma_u^+) = 0.78 \pm 0.02$ eV. Peak H lies 0.244 eV (1970 cm^{-1}) from peak G, and could be assigned to the 1_0^1 transition of the $^3\Sigma_u^+$ state or the origin of the $^3\Pi_g$ state. The latter assignment is favored due to the small but significant difference in the anisotropy parameters for peaks G and H, yielding $T_0(^3\Pi_g) = 1.03 \pm 0.02$ eV.

V. CONCLUSIONS

From the photoelectron spectra of C_4^-, C_6^-, and C_8^- and measurements of the photoelectron angular distributions, we have mapped out many of the low-lying electronic states of C_4, C_6, and C_8 and have obtained new vibrational frequencies for some of these states. These assignments are facilitated by comparisons with *ab initio* calculations. The electronic states we have observed include the $^1\Delta_g$ and $^1\Sigma_g^+$ states, which are derived from the same molecular orbital configuration as the $^3\Sigma_g^-$ ground state, as well as several additional triplet and singlet states lying less than 1.5 eV above the electronic ground state of the neutral clusters. The spectra show that the $^3\Sigma_g^- - ^1\Delta_g$ splitting becomes smaller as the chain length increases. Also, each of the transitions to the various neutral electronic states is dominated by the vibrational origin, indicating relatively small geometry changes upon photodetachment. On the basis of the new spectra, our original assignment of the vibrational frequencies of the C_6 ground state have been modified and are now in much better agreement with *ab initio* values.

All of the excited states seen in this study occur at lower excitation energies than the optical transitions seen by Maier and co-workers.[13,15] In addition, most of the states seen here are optically inaccessible from the $^3\Sigma_g^-$ ground states. However, transitions to the $^3\Pi_u$ excited states in C_4 and C_6, with assigned term values of 0.93 and 1.10 eV, respectively, are optically allowed. It will therefore be of interest to see if these transitions can be located in gas phase or matrix isolation spectroscopy studies of these clusters.

ACKNOWLEDGMENT

This work is supported by the National Science Foundation under Grant No. DMR-9521805.

[1] W. Weltner and R. J. Van Zee, Chem. Rev. **89**, 1713 (1989).
[2] N. Moazzen-Ahmadi, A. R. W. McKellar, and T. Amano, Chem. Phys. Lett. **157**, 1 (1989).
[3] N. Moazzen-Ahmadi, A. R. W. McKellar, and T. Amano, J. Chem. Phys. **91**, 2140 (1989).
[4] P. F. Bernath, K. H. Hinkle, and J. J. Keady, Science **244**, 562 (1989).
[5] J. R. Heath and R. J. Saykally, J. Chem. Phys. **94**, 3271 (1991).
[6] H. J. Hwang, A. Vanorden, K. Tanaka, E. W. Kuo, J. R. Heath, and R. J. Saykally, Mol. Phys. **79**, 769 (1993).
[7] J. R. Heath and R. J. Saykally, in *On Clusters and Clustering, from Atoms to Fractals*, edited by P. J. Reynolds (Elsevier, Amsterdam, 1993), pp. 7–21.
[8] T. F. Giesen, A. Van Order, H. J. Hwang, R. S. Fellers, R. A. Provencal, and R. J. Saykally, Science **265**, 756 (1994).
[9] D. W. Arnold, S. E. Bradforth, T. N. Kitsopoulos, and D. M. Neumark, J. Chem. Phys. **95**, 8753 (1991).
[10] C. C. Arnold, Y. X. Zhao, T. N. Kitsopoulos, and D. M. Neumark, J. Chem. Phys. **97**, 6121 (1992).
[11] C. C. Arnold and D. M. Neumark, J. Chem. Phys. **99**, 1442 (1993).
[12] A. E. Douglas, Nature **269**, 130 (1977).
[13] D. Forney, J. Fulara, P. Freivogel, M. Jakobi, D. Lessen, and J. P. Maier, J. Chem. Phys. **103**, 48 (1995).
[14] D. Forney, P. Freivogel, M. Grutter, and J. P. Maier, J. Chem. Phys. **104**, 4954 (1996).
[15] P. Freivogel, J. Fulara, M. Jakobi, D. Forney, and J. P. Maier, J. Chem. Phys. **103**, 54 (1995).
[16] D. H. Magers, R. J. Harrison, and R. J. Bartlett, J. Chem. Phys. **84**, 3284 (1986).
[17] C. Liang and H. F. Schaefer III, Chem. Phys. Lett. **169**, 150 (1990).
[18] V. Parasuk and J. Almlöf, J. Chem. Phys. **94**, 8172 (1991).
[19] G. Pacchioni and J. Koutecký, J. Chem. Phys. **88**, 1066 (1988).
[20] L. Adamowicz, Chem. Phys. **156**, 387 (1991).
[21] V. Parasuk and J. Almlöf, J. Chem. Phys. **91**, 1137 (1989).
[22] S. H. Yang, C. L. Pettiette, J. Conceicao, O. Cheshnovsky, and R. E. Smalley, Chem. Phys. Lett. **139**, 233 (1987).
[23] S. Yang, K. J. Taylor, M. J. Craycraft, J. Conceicao, C. L. Pettiette, O. Cheshnovsky, and R. E. Smalley, Chem. Phys. Lett. **144**, 431 (1988).
[24] R. F. Liu and X. F. Zhou, J. Chem. Phys. **99**, 1440 (1993).
[25] S. Schmatz and P. Botschwina, Chem. Phys. Lett. **235**, 5 (1995).
[26] R. B. Metz, A. Weaver, S. E. Bradforth, T. N. Kitsopoulos, and D. M. Neumark, J. Phys. Chem. **94**, 1377 (1990).
[27] D. L. Osborn, D. J. Leahy, D. R. Cyr, and D. M. Neumark, J. Chem. Phys. **104**, 5026 (1996).
[28] R. E. Continetti, D. R. Cyr, and D. M. Neumark, Rev. Sci. Instrum. **63**, 1840 (1992).
[29] G. Markovich, R. Giniger, M. Levin, and O. Cheshnovsky, J. Chem. Phys. **95**, 9416 (1991).
[30] V. I. Karataev, B. A. Mamirin, and D. V. Shmikk, Zh. Tekh. Fiz. **41**, 1498 (1971).
[31] B. A. Mamyrin, V. I. Karataev, D. V. Shmikk, and V. A. Zagulin, Zh. Eksp. Teor. Fiz. **64**, 82 (1973).
[32] W. C. Wiley and I. H. McLaren, Rev. Sci. Instrum. **26**, 1150 (1955).
[33] B. A. Mamyrin and D. V. Shmikk, Zh. Eksp. Teor. Fiz. **76**, 1500 (1979).
[34] J. Cooper and R. N. Zare, in *Lectures in Theoretical Physics*, Vol. XI-C, edited by S. Geltman, K. T. Mahanthappa, and W. E. Brittin (Gordon and Breach, New York, 1969), pp. 317–337.
[35] GAUSSIAN 92, M. J. Frisch, G. W. Trucks, M. Head-Gordon, P. M. W. Gill, M. W. Wong, J. B. Foresman, B. G. Johnson, H. B. Schlegel, M. A. Robb, E. S. Replogle, R. Gomperts, J. L. Andres, K. Raghavachari, J. S. Binkley, C. Gonzalez, R. L. Martin, D. J. Fox, D. J. Defrees, J. Baker, J. J. P. Stewart, and J. A. Pople (Gaussian, Inc., Pittsburgh, 1992).
[36] J. D. Watts, I. Cernusak, and R. J. Bartlett, Chem. Phys. Lett. **178**, 259 (1991).
[37] L. Adamowicz, Chem. Phys. Lett. **182**, 45 (1991).
[38] J. D. Watts and R. J. Bartlett, J. Chem. Phys. **97**, 3445 (1992).
[39] K. J. Reed, A. H. Zimmerman, H. C. Anderson, and J. I. Brauman, J. Chem. Phys. **64**, 1368 (1976).
[40] J. Cooper and R. N. Zare, J. Chem. Phys. **48**, 942 (1968).
[41] C. Xu, T. R. Taylor, and D. M. Neumark (unpublished results).
[42] J. Kurtz and L. Adamowicz, Astrophys. J. **370**, 784 (1991).
[43] J. M. L. Martin, J. P. Francois, and R. Gijbels, J. Comput. Chem. **12**, 52 (1991).
[44] J. M. L. Martin, J. P. Francois, and R. Gijbels, J. Chem. Phys. **94**, 3753 (1991).
[45] J. D. Watts and R. J. Bartlett, J. Chem. Phys. **101**, 409 (1994).
[46] S. Schmatz and P. Botschwina, Int. J. Mass. Spec. Ion. Proc. **150**, 621 (1995).
[47] J. M. L. Martin, J. P. Francois, and R. Gijbels, J. Chem. Phys. **93**, 8850 (1990).
[48] J. Hutter, H. P. Luthi, and F. Diederich, J. Am. Chem. Soc. **116**, 750 (1994).
[49] S. Schmatz and P. Botschwina, Chem. Phys. Lett. **245**, 136 (1995).